International Journal of Engineering & Applied Sciences (IJEAS)
Vol.4, Issue 2(2012)59-66

BUCKLING LOAD AND POST-BUCKLING SOLUTION FOR MODE SHAPE OF DELAMINATED BEAM

L.Chattopadhyay[1] and P.K. Jain[2]
[1]*Structural Technologies Division, CSIR-National Aerospace Laboratories, Bangalore 560017*
[2]*B.E (Hons.) Mechanical, Birla Institute of Technology and Science, Pilani, Hyderabad 500078*
Corresponding author: lalitha@nal.res.in

Accepted Date: 12 September 2012

Abstract

This paper presents elastic buckling and post-buckling analysis of an axially loaded isotropic beam-plate with an across-the- width delamination located at a given depth, subjected to in-plane compression. A simple analytical model for determining the global buckling load of the plate with delamination and the mode shape is developed, for various delamination depths and lengths. The influence of applied load on the displacement for a given crack length and depth is studied in the post-buckling state where the non-linear large rotations are included. It is observed that the global buckling load for local delamination buckling increases with the increase in delamination depth from the upper surface, for a given delamination length, and the buckling load decreases if delamination length increases for a given delamination depth. In the post buckling analysis the displacement increases as the applied load increases.

Keywords: Delamination, beam-plate, mode shape, buckling load

a : Spanwise location of crack
b : Crack length
đ**3** : depth from the upper surface
đ**2** : depth from the lower surface
đ: depth of beam
l : Length of beam
b = ***b*** /***l*** (non-dimensional)
a = ***a*** /***l*** (non-dimensional)
d_2 = ***đ*****2**/***đ*** (non-dimensional)
d_3 = ***đ*****3**/***đ*** (non-dimensional)
P_i : applied compressive load in i^{th} region
D_i: flexural rigidity of i^{th} region
w_i : transverse deflection of i^{th} beam
A_{ci} : Area of cross-section of i^{th} region

1. Introduction

The delamination phenomenon of composite materials is one of the most common modes of failure in composite structures and hence it plays a crucial role in assessing the compressive response of structures. The damage induced by such a phenomenon can significantly reduce the buckling strength of the composite.

A delamination in a laminated composite may buckle under compressive loads which causes high inter-laminar stresses at the delamination front and may grow under such conditions. The instability related delamination growth mechanism is a post-buckling process. This post-buckling behavior of a plate depends on the in-plane dimensions, the flexural and in-plane stiffness. The case of one-dimensional delamination is studied on the basis of Euler-Bernoulli theory of beam-plates in [1] and [2]. The deformation of delaminated composites under axial compression is analyzed in [3] using a onedimensional model which is based on the perturbation technique and accounts for transverse shear effects. Strain energy release rate was computed in [4] using system compliance relation and also by finite element approach. Chen studied the elastic buckling and post-buckling analysis of an axially loaded beam- plate having an across-the-width delamination by a variation principle [5]. Buckling analysis of delaminated composite plates by the application of differential quadrature method is given in [6]. A one-dimensional mathematical model was developed in [7] to analyze the buckling behavior of a two-layer beam of two different materials and having asymmetric delamination under clamped boundary conditions. In the present analysis, a layered isotropic elastic beam-plate of unit width and given length with a single delamination at a given depth d_3 from the top surface of the plate is considered. The plate is assumed to be clamped on both the edges and subjected to an axial compressive force **P** at the clamped ends. The delamination is thin line segment and extends across the entire plate width. The geometry of the one dimensional delaminated beam plate is shown in Fig. 1. The co-ordinates used to develop the equations are the local co-ordinates with respect to individual region. In the present work an analytical technique for the determination of global buckling load for local delamination buckling and the mode shape are calculated using continuity conditions, boundary conditions and axial compatibility conditions. The influence of delamination depth and delamination length on the buckling load is studied.

2. Global buckling load for local buckling in a delaminated beam

The beam is considered to comprise of four Euler beams -1, 2, 3, 4, regions 1 and 4 being the integral beams and region 3 and 2 being the delamination region above and below the crack respectively. The part above the delamination plane is referred to as the `upper' sub-laminate, and the part below it is referred to as the `lower' sub-laminate. The sections before and after delamination, where the plate is intact are referred to as the `base' laminate. Q_i and M_i are the shear force and the bending moments of the i^{th} region at the crack tip.

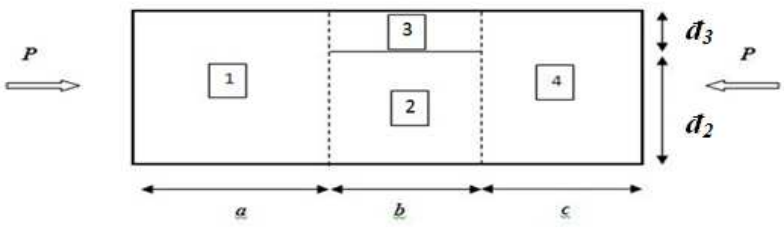

Figure 1: Beam subjected to compressive load

The governing equations for buckling in the i^{th} region is given by

$$\frac{\partial^4 w_1}{\partial x^4} + \lambda_i^2 \frac{\partial^2 w_1}{\partial x^2} = 0 \qquad i = 1, 2, 3, 4 \tag{1}$$

A general solution for all the beams is written as

$$w_i(x) = A_{1i}\sin(\lambda_i x) + A_{2i}\cos(\lambda_i x) + A_{3i}x + A_{4i} \qquad i = 1, 2, 3, 4 \tag{2}$$

Where,

$$\lambda_i = \sqrt{\frac{P_i}{D_i}} \tag{3}$$

$A_{1i}, A_{2i}, A_{3i}, A_{4i}$, are arbitrary constants. In the present analysis, the normalized applied load is given by,

$$\bar{P} = \frac{P_1}{4\pi^2 D_1} \tag{4}$$

Boundary conditions at the clamped edges are given by,

$$\left.\begin{aligned} w_1(0) &= 0 \\ w_4(0) &= 0 \\ \frac{\partial w_1}{\partial x}|_{x=0} &= 0 \\ \frac{\partial w_4}{\partial x}|_{x=0} &= 0 \end{aligned}\right\} \tag{5}$$

Displacement continuity conditions at the delamination tip are given by,

$$\left.\begin{aligned} w_1(a) &= w_2\left(-\frac{b}{2}\right) \\ w_1(a) &= w_3\left(-\frac{b}{2}\right) \\ w_4(-c) &= w_2\left(\frac{b}{2}\right) \\ w_4(-c) &= w_3\left(\frac{b}{2}\right) \end{aligned}\right\} \tag{6}$$

Slope continuity conditions at the delamination tip are given by

$$\left.\begin{aligned} \frac{\partial w_1}{\partial x}|_{x=a} &= \frac{\partial w_2}{\partial x}|_{x=-\frac{b}{2}} \\ \frac{\partial w_1}{\partial x}|_{x=a} &= \frac{\partial w_3}{\partial x}|_{x=-\frac{b}{2}} \\ \frac{\partial w_4}{\partial x}|_{x=-c} &= \frac{\partial w_2}{\partial x}|_{x=\frac{b}{2}} \\ \frac{\partial w_4}{\partial x}|_{x=-c} &= \frac{\partial w_3}{\partial x}|_{x=\frac{b}{2}} \end{aligned}\right\} \tag{7,8}$$

Shear force continuity conditions are given by,

$$Q_1 = Q_2 + Q_3$$

$$\gg \quad \frac{\partial^3 w_1}{\partial x^3}\Big|_{x=a} = (d_2^3)\frac{\partial^3 w_2}{\partial x^3}\Big|_{x=-\frac{b}{2}} + (d_3^3)\frac{\partial^3 w_3}{\partial x^3}\Big|_{x=-\frac{b}{2}}$$

$$Q_4 = Q_2 + Q_3$$

$$\gg \quad \frac{\partial^3 w_4}{\partial x^3}\Big|_{x=-c} = (d_2^3)\frac{\partial^3 w_2}{\partial x^3}\Big|_{x=\frac{b}{2}} + (d_3^3)\frac{\partial^3 w_3}{\partial x^3}\Big|_{x=\frac{b}{2}} \qquad (9)$$

Continuity conditions of bending moment at the delamination tip are given by,

$$M_1 = M_2 + M_3 + \frac{P_3 d_2}{2} - \frac{P_2 d_3}{2}$$

$$\gg \quad \frac{\partial^2 w_1}{\partial x^2}\Big|_{x=a} = (d_2^3)\frac{\partial^2 w_2}{\partial x^2}\Big|_{x=-\frac{b}{2}} + (d_3^3)\frac{\partial^2 w_3}{\partial x^2}\Big|_{x=-\frac{b}{2}} - \frac{1}{2}\left(\frac{P_2 L^2 d_3}{D_1} - \frac{P_3 L^2 d_2}{D_1}\right) \qquad (10)$$

$$M_4 = M_2 + M_3 + \frac{P_2 d_3}{2} - \frac{P_3 d_2}{2}$$

$$\gg \quad \frac{\partial^2 w_4}{\partial x^2}\Big|_{x=-c} = (d_2^3)\frac{\partial^2 w_2}{\partial x^2}\Big|_{x=\frac{b}{2}} + (d_3^3)\frac{\partial^2 w_3}{\partial x^2}\Big|_{x=\frac{b}{2}} + \frac{1}{2}\left(\frac{P_2 L^2 d_3}{D_1} - \frac{P_3 L^2 d_2}{D_1}\right) \qquad (11)$$

Axial compatibility condition is given by,

$$\frac{d}{2}\left(\frac{\partial w_1}{\partial x}\Big|_{x=a} - \frac{\partial w_4}{\partial x}\Big|_{x=-c}\right) = \left\{-\frac{P_3 b}{E\,A_{c3}} - \frac{d}{2}\int_{-\frac{b}{2}}^{\frac{b}{2}}\left(\frac{\partial w_3}{\partial x}\right)^2 dx\right\} - \left\{-\frac{P_2 b}{E\,A_{c2}} - \frac{d}{2}\int_{-\frac{b}{2}}^{\frac{b}{2}}\left(\frac{\partial w_2}{\partial x}\right)^2 dx\right\} \qquad (12)$$

When buckling occurs, the non-linear terms do not have any contribution and hence the above equation reduces to:

$$\frac{d}{2}\left(\frac{\partial w_1}{\partial x}\Big|_{x=a} - \frac{\partial w_4}{\partial x}\Big|_{x=-c}\right) = \left\{-\frac{P_2 b}{E\,d_2}\right\} - \left\{-\frac{P_3 b}{E\,d_3}\right\} \qquad (13)$$

Q_i and M_i are the shear force and the bending moments of the i^{th} region at the crack tip. From the above equations (11-13) a 16x16 matrix of the form [A][X] = 0 is obtained. For a non-trivial solution to exist, the determinant must vanish. Thus, equating |A|=0, the lowest Eigen value is obtained by solving transcendental equation.

3. Results of the buckling analysis

The following data is obtained for the buckling load normalized with respect to Euler load. This is compared with other references and validation is confirmed. Table 1. gives the normalized buckling load for a central delamination for various values of crack length (b).

For a fixed depth from the top surface (d_3), as the crack length increases buckling load decreases and the buckling load increases as the crack moves away from the top surface. Table 2 gives the buckling load for a particular depth and different crack lengths and the results are in good agreement with the literature values [8.9,10]. The buckling load plot for various crack lengths (b) and different heights (d_3) from the top surface is shown in Fig.2.

Table 1: Normalized Buckling load for central delamination

d_3	b = 0.1	b = 0.3	b = 0.5	b = 0.7	b = 0.9
0.1	0.979922	0.110943	0.039959	0.020396	0.012343
0.2	0.999714	0.437109	0.158547	0.081221	0.049304
0.3	0.999825	0.858225	0.346905	0.180355	0.110496
0.4	0.999859	0.954327	0.567541	0.311104	0.194872
0.5	0.999868	0.96383	0.689563	0.430967	0.293302

Table 2: Comparison of buckling load for different crack lengths (d_3= *0.2)*

Crack length (b)	Present value	Reference value[8]	Reference value[9]	Reference value[10]
0.1	0.999714	0.99966	0.9997	0.99971
0.3	0.437108	0.43712	0.4371	0.43711
0.5	0.158546	0.15855	0.1585	0.15855
0.7	0.081221	0.08122	0.0812	0.08122
0.9	0.049304	0.04930	0.0493	0.04930

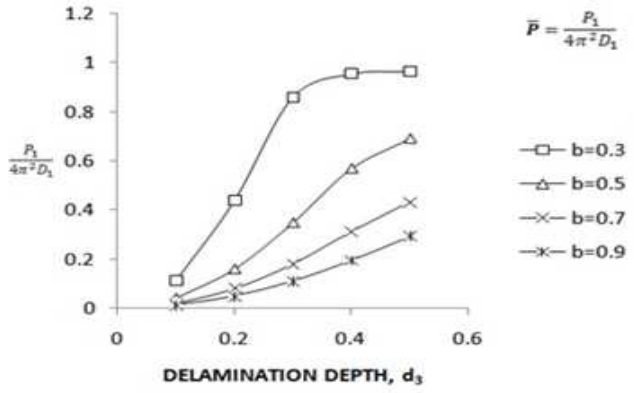

Figure 2: Buckling load vs. delamination depth

4. Post-buckling solution and delamination mode shape

The post-buckling case for the isotropic beam with the same assumptions as earlier will be dealt, considering the fact that the delamination is centrally located. Hence in the present

case $a = c = \frac{l-b}{2}$. The displacements are obtained from the governing buckling equation and they are given by,

$$w_1(x) = B\left(1 - \cos\left[\lambda_1\left(\frac{l}{2} - x\right)\right]\right)$$

$$w_2(x) = B\left\{\left(\frac{\lambda_1 \sin\left[\lambda_1\left(\frac{l}{2} - \frac{b}{2}\right)\right]}{\lambda_2 \sin\left[\frac{\lambda_2 b}{2}\right]}\right)\left(\cos[\lambda_2 x] - \cos\left[\frac{\lambda_2 b}{2}\right]\right) + 1 - \cos\left[\lambda_1\left(\frac{l}{2} - \frac{b}{2}\right)\right]\right\} \quad (15)$$

$$w_3(x) = B\left\{\left(\frac{\lambda_1 \sin\left[\lambda_1\left(\frac{l}{2} - \frac{b}{2}\right)\right]}{\lambda_3 \sin\left[\frac{\lambda_3 b}{2}\right]}\right)\left(\cos[\lambda_3 x] - \cos\left[\frac{\lambda_3 b}{2}\right]\right) + 1 - \cos\left[\lambda_1\left(\frac{l}{2} - \frac{b}{2}\right)\right]\right\} \quad (16)$$

The amplitude B, λ_2 and λ_3 are calculated for a given applied load P by using the force equation, moment equation, axial compatibility equation.

The force equation is given by,

$$P_1 = P_2 + P_3 \quad (17)$$

The moment equation is given by,

$$M_1 = M_2 + M_3 + \frac{P_3 d_2}{2} - \frac{P_2 d_3}{2}$$

$$\gg \quad D_1 \left.\frac{\partial^2 w_1}{\partial x^2}\right|_{x = b/2} = D_2 \left.\frac{\partial^2 w_2}{\partial x^2}\right|_{x = \frac{b}{2}} + D_3 \left.\frac{\partial^2 w_3}{\partial x^2}\right|_{x = \frac{b}{2}} - \left(\frac{P_2 d_3}{2} - \frac{P_3 d_2}{2}\right) \quad (18)$$

The axial compatibility equation is given by,

$$\frac{P_3 b}{2 E d_3} + \frac{1}{2}\int_0^{\frac{b}{2}}\left(\frac{\partial w_3}{\partial x}\right)^2 dx - \frac{P_2 b}{2 E d_2} - \frac{1}{2}\int_0^{\frac{b}{2}}\left(\frac{\partial w_2}{\partial x}\right)^2 dx = \frac{d_2 + d_3}{2}\left.\frac{\partial w_3}{\partial x}\right|_{x = \frac{b}{2}} \quad (19)$$

Substituting the displacement equations w_1,w_2 and w_3 as defined in (19-21)and substituting P_1, P_2 and P_3 in terms of the eigen values, as defined by,

$$P_i = \lambda_i^2 D_i \quad (20)$$

we obtain three equations, with variables B, λ_2 and λ_3. The above variables are solved for every value of input force and the individual displacement fields are obtained. Consequently, the mode shape is generated. The following table gives normalized applied load for a given delamination length and the delamination depth from the top surface of the beam. Table 3 gives the numerical values for displacement and amplitude for a given crack length and depth from the top surface. Fig.3 gives the graph for the upper and lower surface displacement for a given crack lengths at different applied load levels in the post-buckling analysis. Table 4 gives upper and lower surface displacement for various applied load when $d_3 << b$ and Fig.4 gives the graph of the displacement when the distance from the top surface is very small (thin film delamination).

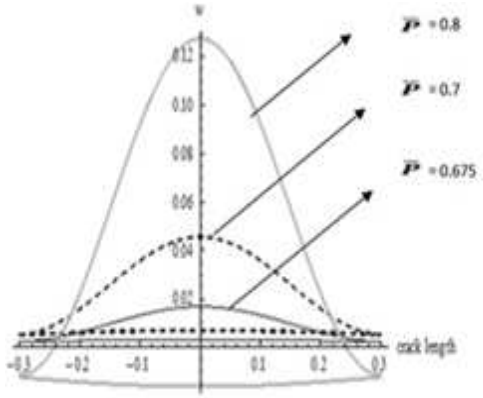

Figure 3: Upper and lower surface displacement vs. crack length for different normalized applied load

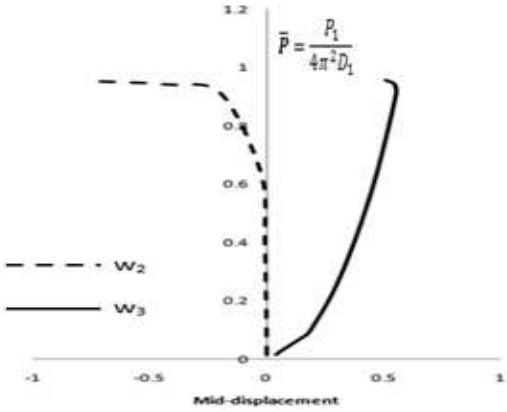

Figure 4. Upper and lower surface displacements vs. applied load when $d_3 \ll b$

Table 3: Normalized upper and lower surface displacement and amplitude for various applied load in post buckling (d_3=0.25 b=0.3)

$\bar{P}$	w_2/ d_3	w_3/ d_3	B
0.675119	0.012688	0.067105	0.001926
0.750375	0.022467	0.377215	0.003196
0.800854	-0.06416	0.51818	-0.00879

Table 4: Normalized upper and lower surface displacement for various applied load when $d_3 \ll b$ (d_3=0.02 b=0.5)

$\bar{P}$	w_2	w_3
0.016228	-0.00013	0.03866
0.025356	-0.00023	0.051473
0.085845	-0.00117	0.171219
0.08791	-0.0012	0.1733
0.088667	-0.00122	0.174056
0.089618	-0.00123	0.175002
0.091535	-0.00126	0.176893
0.101424	-0.00142	0.186342
0.228204	-0.00378	0.280433
0.405696	-0.00891	0.37408
0.6339	-0.02354	0.46724
0.912816	-0.19737	0.551977
0.943497	-0.42883	0.542373

5. Conclusions

A simple analytical method is developed for the buckling load and mode shape for an isotropic delaminated beam. It has been observed that in the buckling analysis, (1) As the delamination depth increases for a given delamination length, the buckling load increases. (2) For a very small delamination, the effect of depth on buckling load is more predominant when the defect is near the surface. (3) For a given depth, buckling load increases as the delamination length gets shorter. (4) For a very long delamination, the critical buckling load is much lesser when compared to other delamination lengths. (5) In calculating the post buckling parameters namely the displacements and amplitude, non-linear terms are included and we observe that the displacement increases as the applied load increases.

References

[1] Chai H., Babcock, C.D and Knauss, W., "One dimensional modeling of failure in laminated plates by delamination buckling", Int..J. Structures, 1981, Vol.17, (11), pp.1069-1083.

[2] Wan-Lee Yin, Wang J.T.S. "The energy release rate in the growth of a one-dimensional delamination", journal of Applied Mechanics, 1984, Vol.51, pp. 939-941.

[3] G. A. Kardomateas and D.W. Schmuesert, "Buckling and post buckling of delaminated composites under compressive loads including transverse shear effects", AIAA Journal, 1988, Vol.26, , pp 337-343.

[4] J.F. Williams, D.C. Stouffer, S.Ilic and R.Jones, "An analysis of delamination behaviour", Composite structures, 1986, Vol.5, pp. 203-216

[5] Chen H P. "Shear deformation theory for compressive delamination buckling and growth", AIAA Journal 1991, Vol.29, (5), pp.813–819.

[6] Moradi S, Taheri F."Application of DQM as an effect solution tool for buckling response of delaminated composite plates", Composite Structures 2001, Vol.51, 439–449.

[7] M S Rao Parlapalli, Dongwei Shu, "Buckling analysis of two-layer beams with an asymmetric delamination" Engineering Structures, 2004, Vol. 26, pp.651–658.

[8] Moradi S, Taheri F. Application of the differential quadrature method to the analysis of delamination buckling of composite beam-plates. In proceedings of the computer modelling and simulations in engineering, International conference on computational engineering science, May 1997, pp. 1238–1243

[9] Simitses, G. J., Sallam, S. & Yin, W. L., Effect of delamination of axially loaded homogeneous laminated plates. A&I4 J., 23 (1985) 1437-1444

[10] Chen, Hsin-Piao, Shear deformation theory for compressive delamination buckling and growth. ALAA J., 29 (1991) 813-819